BNL-219092-2020-TECH
ASC-PW-2004

Magnetic Field Measurements for Fast-Changing Magnetic Fields

A. Marone

Superconducting Magnet Division
Brookhaven National Laboratory

U.S. Department of Energy
USDOE Office of Science (SC), Nuclear Physics (NP) (SC-26)

DISCLAIMER

Magnetic Field Measurements For Fast-Changing Magnetic Fields

Animesh Jain, John Escallier, George Ganetis, Wing Louie, Andrew Marone, Richard Thomas, Peter Wanderer

***Abstract*—Several recent applications for fast ramped magnets have been found that require rapid measurement of the field quality during the ramp. (In one instance, accelerator dipoles will be ramped at 1 T/sec, with measurements needed to the accuracy typically required for accelerators.) We have built and tested a new type of magnetic field measuring system to meet this need. The system consists of 16 stationary pickup windings mounted on a cylinder. The signals induced in the windings in a changing magnetic field are sampled and analyzed to obtain the field harmonics. To minimize costs, printed circuit boards were used for the pickup windings and a combination of amplifiers and ADC's used for the voltage readout system. New software was developed for the analysis. Magnetic field measurements of a model dipole developed for the SIS200 accelerator at GSI are presented. The measurements are needed to insure that eddy currents induced by the fast ramps do not impact the field quality needed for successful accelerator operation.**

***Index Terms*—Fast ramped magnets, Facility for Antiproton and Ion Research, magnetic field measurement, superconducting accelerator magnets.**

I. Introduction

WE have undertaken the development of a precise magnetic field measuring system for measuring magnets which will operate at high ramp rates (e.g., 1 T/s). High ramp rates are part of the design of the SIS100 and SIS300 rings to be built as part of the Facility for Antiproton and Ion Research (FAIR) [1], for J-PARC [2], and for a proposed upgrade of the AGS at BNL [3]. Another application is to magnets built to vary the field of NMR magnets so that the motion of awake animals can be tracked [4]. This paper reports the first set of measurements made with this system. The measurements were made on a model magnet built as part of the R&D for the SIS 200 ring at FAIR. The FAIR design now calls for a higher-energy ring, SIS300 [5].

Manuscript received October 5, 2004. This work was supported in part by the U.S. Department of Energy under contract number DE-AC02-98CH10886 and in part by Gesellschaft fur Schwerionen Physik (GSI).

The authors are with the Superconducting Magnet Division, Brookhaven National Laboratory, PO Box 5000, Upton NY 11973. Their other contact information is:

A. Jain (phone 1 631 344 7329, fax 1 631 344 2190, email: jain@bnl.gov).
G. Ganetis (ganetis1@bnl.gov)
W. Louie (louie@bnl.gov)
A. Marone (andym@bnl.gov)
R. Thomas (thomas1@bnl.gov)
P. Wanderer (wanderer@bnl.gov)

II. Magnet Construction

The model magnet (Fig. 1) was built using RHIC [6] and BNL/LHC [7] magnet tooling and components modified to accommodate the requirement for fast ramped magnets. Previous papers have reported details of the magnet construction and quench tests [8] and energy loss measurement [5]. The construction is briefly recounted below, with emphasis on changes made to the basic RHIC and BNL/LHC designs to permit fast ramping.

A. Superconductor

The strand used for the cable has diameter 0.641 mm and J_c ~ 2900 A/mm^2 (5 T, 4.2 K, measured via transport current). The strand is coated with Staybrite. Two 25 μm thick, 8 mm wide stainless steel cores were inserted in the cable as it was formed. The cable was insulated with two wraps of Kapton®, each 25 μm thick, with 50% overlap of each wrap and with polyimide adhesive. A laser was used to cut cooling holes in the insulation on the thin edge of the insulated cable.

B. Magnet

When feasible, this magnet used components made from insulators rather than metals. For example, the three wedges used in the coil were G11. Each half coil is 0.035" (0.89 mm) larger in the azimuthal dimension than RHIC coils, due to the stainless steel cores in the cable. To accommodate the coil

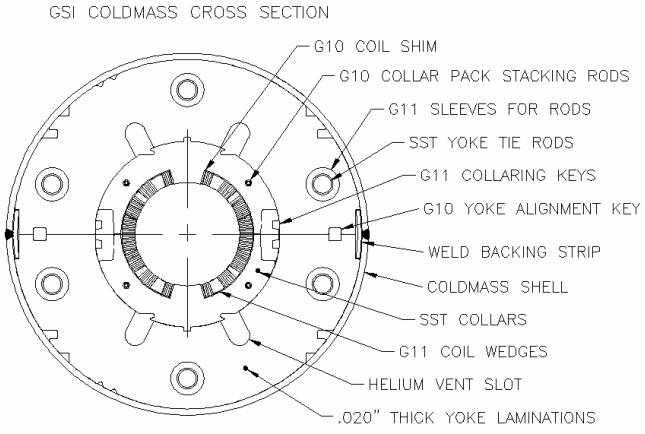

Fig. 1. Cold mass cross section. The coil i.d. is 8 cm.

oversize, the thickness of the G10 pole shim was reduced. The coils were collared with Kawasaki high-Mn stainless steel collars. The yoke laminations were 0.5 mm thick, low coercivity steel (H_c = 31 A/m) with 3.3% Si. Further details are given in [8].

III. Construction of Measurement Coil

We have developed a harmonic coil array for measuring fast-ramped magnets. Printed circuits are relatively inexpensive and reproducible, and are used for the windings. Sixteen printed circuits are mounted as tangential coils on a cylinder. We are sampling terms as high as the 16-pole, with the goal of obtaining reliable measurements at least as high as the decapole. The 16 probes were intercalibrated by rotating the coil in a reference dipole field [9]. However, the coil will be stationary when used for measuring fast-ramped fields.

The voltage can be sampled at rates as high as 10 kHz. The voltage sampling system also covers a wide range of signal amplitudes and allows for frequent calibration and DC offset checks.

In the stationary mode, the total flux seen by a given probe is determined by its angular position, as well as the multipole components of the field. The angular profile constructed with voltage signals from various probes is, in general, not a Fourier series.

For this magnet, we use a 10-layer printed circuit board with six turns per layer for a total of 60 turns. The lines on the circuit boards are 0.1 mm wide and have 0.1 mm gaps between them. The circuit boards are 0.3 m long and the average width of the pattern is 8.2 mm. The boards are 1.6 mm thick and the effective radius of the cylinder on which the probes are mounted is 26.8 mm. Fig. 2 shows the probe array assembled for this magnet. The fractional rms variation of the response of the boards mounted on the coil is 10^{-4}.

Fig. 2. The array of 16 printed circuits mounted on the cylindrical coil form used for fast-ramp measurements of the GSI magnet. The printed circuits are 300 mm long.

IV. Data Acquisition System

We are using 16-bit commercial ADC's and custom-built programmable gain amplifiers to obtain the factor of ~ 100 needed for some of the measurements. For stability, the amplifiers have been mounted in a temperature-controlled box. The approximate offsets and amplifier gain corrections are obtained typically once a day by applying known signals to all the input channels for each of the 16 amplifier gain/ADC range combinations. For each ramp, the offsets are calculated during the time at constant current that immediately precedes the ramp.

V. Data Analysis

For the purpose of data analysis, a coordinate system internal to the coil is used. The X-axis is chosen along the centerline of one of the probes, as shown in Fig. 3. Since the relative angles of all the probes are determined by rotating the coil in a dipole field, the angular positions, θ_i, of all the probes are known in this coordinate system. In practice, it is desirable to align this coordinate system as best as possible with the magnet's principal axes. A perfect alignment, however, is not essential, and will not be assumed in the data analysis.

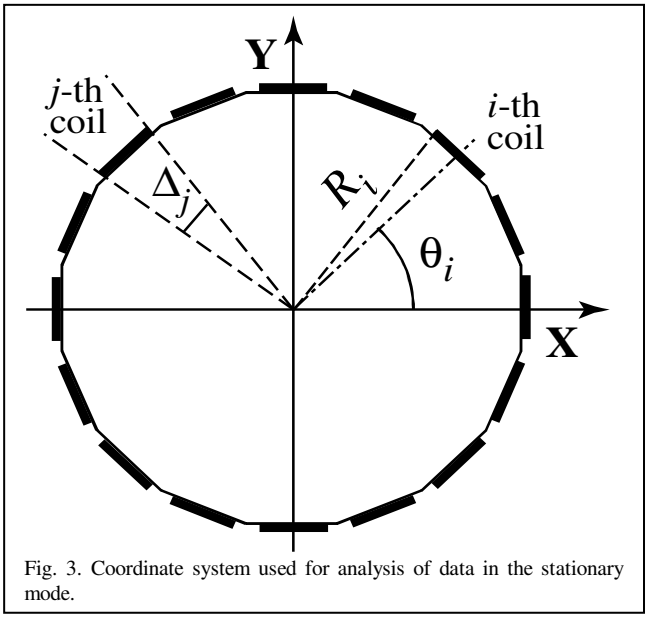

Fig. 3. Coordinate system used for analysis of data in the stationary mode.

The flux linked at time t through the i-th tangential coil of length L_i and having N_i turns is given by

$$\Phi_i(t) = \sum_{n=1}^{\infty} \frac{2N_i L_i R_{ref}}{n} \left(\frac{R_i}{R_{ref}}\right)^n \sin\left(\frac{n\Delta_i}{2}\right) \times \left[B_n(t)\sin(n\theta_i) + A_n(t)\cos(n\theta_i)\right] \quad (1)$$

where $B_n(t)$ and $A_n(t)$ are the normal and skew $2n$-pole terms respectively at a reference radius of R_{ref} in a harmonic expansion of the 2-D field components. The induced voltage in the i-th probe in the stationary mode results from a time variation of the field components, and is given by

$$V_i(t) = \sum_{n=1}^{\infty} \frac{2N_i L_i R_{ref}}{n} \left(\frac{R_i}{R_{ref}}\right)^n \sin\left(\frac{n\Delta_i}{2}\right) \times \left[\dot{B}_n(t)\sin(n\theta_i) + \dot{A}_n(t)\cos(n\theta_i)\right] \quad (2)$$

where the dot over B_n and A_n denotes time derivative. In a conventional rotating tangential coil, a complete angular profile is obtained by rotating the *same* coil. All the geometric parameters in this case are angle independent, and the expression for the flux, or the voltage, represents a Fourier series. In the case of an array of tangential coils in the stationary mode, the geometric parameters are not necessarily

the same for all the coils. Consequently, the various terms in the summation in (1) or (2) are *not* the same as the Fourier components of the voltage profile. Thus, a simple FFT analysis of the voltage profile assembled from the signals of all the probes does not directly give the harmonic terms.

In our analysis, we obtain the time derivatives of the 16 lowest-order harmonics (normal and skew, dipole through 16-pole) by solving the 16 linear equations which link the measured voltages and the harmonics (see Eq. 2).

The harmonic components at any time are obtained by integrating the time derivatives:

$$B_n(t) = B_n(0) + \int_0^t \dot{B}_n(t)\,dt; \quad A_n(t) = A_n(0) + \int_0^t \dot{A}_n(t)\,dt \qquad (3)$$

The initial values of the harmonics, $B_n(0)$ and $A_n(0)$, are determined using the same coil in a rotating mode before the magnet is ramped. After this measurement, the coil is aligned with the frame used for the rotating mode data, as defined by the index pulse of the angular encoder. The numerical integration can be avoided if one uses digital integrators instead of voltmeters to record the probe signals.

VI. Magnetic Field Measurement

For this first test, we report a measurement of the normal sextupole generated by the ramping of the magnet. We began by making DC measurements with an existing rotating coil system and with the new system operating in the rotating mode. The DC measurement of the geometric sextupole by the new system, -37 units, is calculated by averaging the up and down ramp measurements given in Table I. (A unit is defined as 10^4 times the harmonic field divided by the fundamental field at a reference radius of 25 mm.) It is in good agreement with the measurement made by the existing system and with a calculation for the magnet with its oversized coil [10]. The existing ~1 m coil is much longer than the new coil and sees some part of the magnet ends, so the two measurements are not directly comparable. Good agreement between calculation and measurement with the new system is found for the first four allowed harmonics. After this measurement, the coil of the new (i.e., fast ramp) system was rotated so that its reference frame was aligned with the frame used for this coil in rotating mode.

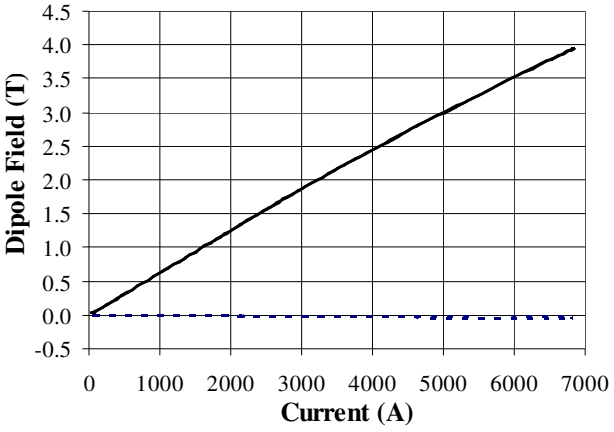

Fig. 4. Normal (solid) and skew (dashed) dipole fields vs. current, ramped at 4900 A/s.

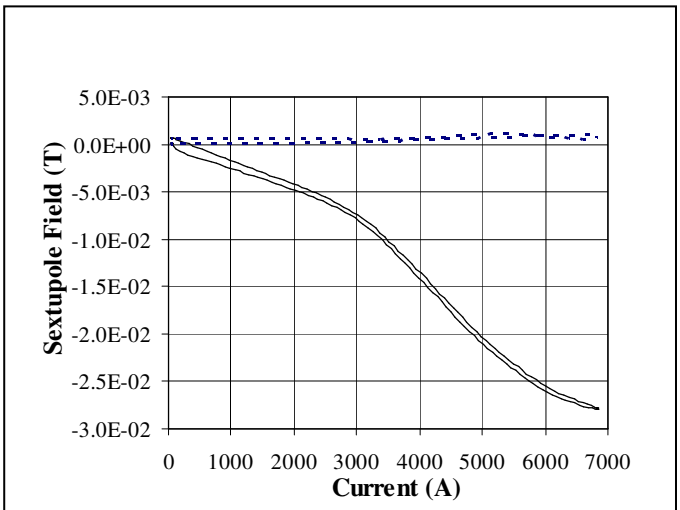

Fig. 5. Normal (solid) and skew (dashed) sextupole fields vs. current, ramped at 4900 A/s.

With the fast ramp coil properly aligned, the magnet was ramped from 50 A (0.03 T) to 6800 A (4T) at 4900 A/s (3 T/s) and then back to 50A at the same rate. Two such ramp cycles were carried out to set up the magnet history before taking data in the third ramp. The offsets of the amplifier/ADC system were measured at constant current (50A) immediately prior to the ramp. The offsets were not measured at the end of the ramping because of the finite decay time of the eddy currents.

TABLE I
NORMAL SEXTUPOLE (UNITS) AT 1 KA (0.6 3T)

dB/dt(T/s)	B_{max}(T)	b_3^U	b_3^D	b_3^D-b_3^U
0	4.3	-40.6	-34.9	5.7
3	4.0	-40.5	-27.4	13.1

Figs. 4 and 5 show the normal and skew dipole and sextupole fields as a function of current, up and down ramp. (At high current, the normal sextupole becomes more negative due to the saturation of the yoke.) There is good point-to-point

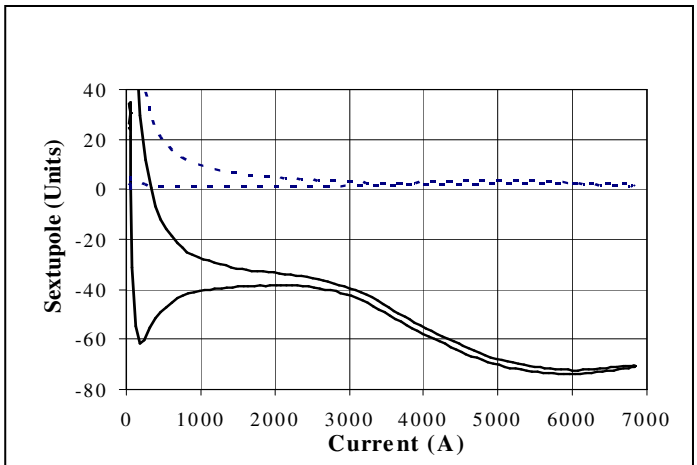

Fig. 6. Normal (solid) and skew sextupole (dashed) vs. current, ramped at 4900 A/s.

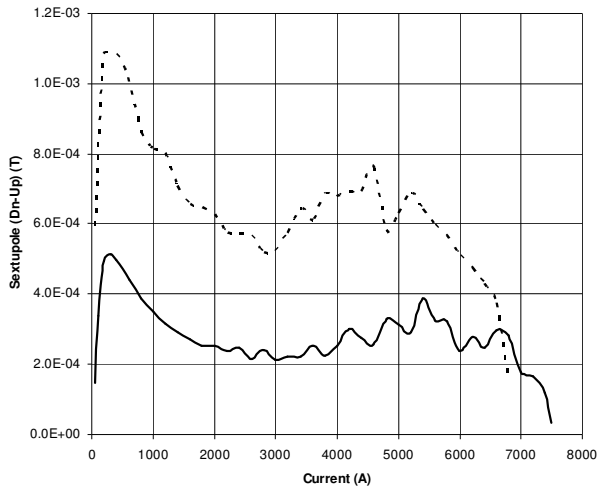

Fig. 7. For DC (solid) and fast ramped (dashed) measurements, the difference (down ramp – up ramp) in sextupole fields versus current.

reproducibility. The fields at the end of the down ramp are close to those at the start of the up ramp, indicating that the offset corrections are nearly correct.

Fig. 6 shows the normal and skew sextupole in units. The normal sextupole displays the usual hysteresis curve. The hysteresis in the skew sextupole may be due to inaccurate offset corrections.

To remove any systematic differences between the DC and AC measurements of the field, we compare the difference down ramp – up ramp (i.e., the width of the hysteresis loop) during the fast ramping to the down-up difference obtained from the DC measurement. The eddy current sextupole will appear at twice its magnitude in the fast-ramp difference but be absent from the DC difference. Fig. 7 shows the differences in the sextupole fields as a function of current for the DC and fast ramp measurements. It is useful to compare the DC and fast ramp differences in the region 1 kA – 2 kA, where the effects of magnetization are modest and the width of the hysteresis loop is much larger than the noise of ~ 1 x 10^{-4} T. The differences at 1 kA are listed in Table I, in units.

From Table I, we see that the width of the hysteresis loop of the normal sextupole is 13.1 units for the fast-ramp measurement and 5.7 units for the DC measurement. Half the difference, 3.7 units, could be attributed to the eddy current sextupole at 1 kA (0.63 T central field) during the up ramp. We estimate that the uncertainty in this measurement of the eddy current sextupole is ~ 2 units. Since the magnetic field produced by the eddy current is constant at constant ramp rate, whereas the central field is roughly linear with current, the eddy current harmonics (in units) will vary inversely with current. For example, at 500A, the eddy current normal sextupole is ~ 7.4 10^{-4}.

The eddy current decapole is estimated to be ~ 2 units, but is not well-determined at the present time.

VII. Conclusion

Initial harmonic measurements of an SIS200 model dipole ramped at the high rate of 3 T/s have been made. The normal sextupole due to the fast ramping is 3.7 units, with an uncertainty of ` 2 10^{-4} units.

Acknowledgment

We are grateful for the contributions of our design and technician staff, B. Azzara, J. Cintorino, J. McNeil, D. Oldham, A. Sauerwald, and D. Sullivan. We thank R. Gupta for his calculation of the geometric field quality.

References

[1] W. Henning, "An international accelerator facility for research with ions and antiprotons," presented at 9th European Particle Accelerator Conference, Lucerne, Switzerland, July 5-9, 2004.

[2] Y. Irie, "Challenges facing the generation of MW proton beams using rapid cycling synchrotrons," presented at 9th European Particle Accelerator Conference, Lucerne, Switzerland, July 5-9, 2004.

[3] N. Tsoupas, *et al.*, "Injection acceleration and extraction of high intensity proton beam for the "Neutrino Facility" project at BNL," *Proc. 2003 Particle Accelerator Conf.*, Portland, pp. 1637-1639. Available: http://accelconf.web.cern.ch/accelconf/p03/PAPERS/TPPB006.PDF

[4] T. Ernst, *et al*., "Imaging the awake animal brain," project underway at Brookhaven National Laboratory, Upton, NY, USA

[5] G. Moritz, "Fast-pulsed SC magnets," presented at 9th European Particle Accelerator Conference, Lucerne, Switzerland, July 5-9, 2004.

[6] M. Anerella et al., "The RHIC magnet system," Nucl. Instrum. Meth. A 499 (2003) pp. 280-315.

[7] J. Muratore et al., "Test results for prototypes of the twin aperture dipoles for the LHC insertion region," IEEE Trans. Applied Superconductivity, vol. 12, no. 1, March 2002, pp. 309-312.

[8] P. Wanderer et al., "Initial test of a fast-ramped superconducting model dipole for GSI's proposed SIS200 accelerator," Proc. 2003 Particle Accelerator Conference, pp. 2162-2162, available at http://accelconf.web.cern.ch/AccelConf/p03/PAPERS/WPAB054.PDF

[9] P. Wanderer et al., "Development of a precise magnetic field measurement system for fast-changing magnetic fields," IEEE Trans. Applied Superconductivity, vol 14., no. 2, June 2004, p. 1826-1829.

[10] R. Gupta, private communication.